

Influence of cross diffusions on natural convection flow through annulus region with Navier slip and convective boundaries

Kolla Kaladhar, Eerala Komuraiah and
Kothakapu Madhusudhan Reddy

Communicated by Valéry Covachev

Abstract. In this manuscript we present the influence of cross diffusions on incompressible natural convection laminar flow between concentric cylinders with slip and convective boundaries. In addition, the first order chemical reaction is also considered. The governing equations with boundary conditions are transformed to a non - dimensional form with suitable transformations. Homotopy Analysis Method (HAM) is used to solve the system of equations. The influence of the various parameters like Slip, Dufour, Soret, chemical reaction parameters and the Biot number on velocity, temperature and concentration are investigated and presented through plots. It is found from this study that the influence of slip parameter and Biot number, the velocity and temperature profiles increase, while there is a reverse tendency under the effect of chemical reaction parameter.

Keywords. Free convection, Navier slip, chemical reaction, cross diffusion effects, convective boundary, HAM.

2010 Mathematics Subject Classification. 76R10, 74F25, 76R50, 65H20.

1 Introduction

Free convection flow with heat and mass transfer in a circular annulus has an incredible significance in various fields [1–4]. In view of applications, Ha and Jung [5] studied three-dimensional conjugate heat transfer of free convection and conduction in a differentially heated cubic enclosure within which a centered heat-conducting body generates heat numerically. The influence of chemical reaction on free convection from vertical surfaces in porous media considering Soret and Dufour effects has been contributed by Postelnicu [6]. Sheikholeslami and Shamlooei [7] simulated the natural convection heat transfer in a cavity with sinusoidal wall filled with CuO - water, numerical simulation and $\text{Fe}_3\text{O}_4 - \text{H}_2\text{O}$ nanofluid in the presence of magnetic field. Most recently, Mehryan et al. [8] investigated the conjugate natural convection of nanofluids inside an enclosure filled by three

layers of solid, porous medium and free nanofluid using Buongiorno's and local thermal non-equilibrium models.

Normally, Soret and Dufour effects are assumed to be negligible in problems related to double diffusive convection. In addition, homogeneous and heterogeneous reactions exist in many chemical reactions. For the past literature and applications, one can refer the work of Ramkissoon and Majumdar [9]. In view of the significance, Ibrahim et al. [10] studied the impact of Soret and chemical reaction on free convection non-Newtonian fluid with yield stress. Makinde et al. [11] studied the chemically-reacting hydromagnetic boundary layer flow with Soret/Dufour effects and a convective surface boundary condition numerically. Srinivasacharya and Kaladhar [12] presented the nature of couple stress fluid in a vertical channel under the influence of cross diffusions and chemical reaction. Nagaraju et al. [13] presented the effects of Soret and Dufour, chemical reaction, Hall and ion currents on magnetized micropolar flow through co-rotating cylinders. The analysis of heat and mass transfer in a natural convection flow of nanofluid over a vertical cone with chemical reaction has been carried out by Reddy and Chamkha [14]. Recently, Jain and Choudhary [16] investigated the Soret and Dufour effects on thermophoretic MHD flow and heat transfer over a non-linear stretching sheet with chemical reaction. Most recently, Nagaraju et al. [15] explained the second law analysis of flow in a circular pipe with uniform suction and magnetic field effects.

In this article, the free convection flow in an annulus with Navier slip condition [17–19] and convective boundary condition [20–23] has been studied along with cross diffusions and first order chemical reaction. Homotopy analysis method (HAM) [24–28] has been applied to get the solution of the present system. The survey clearly showed that the combined effects with slip flow condition and the convective boundary with cross diffusion in an annulus region have not been reported by any researcher. In view of its significance, the authors are motivated to take this problem. Finally, the variation of flow components with respect to the emerging parameters were discussed.

2 Formulation of the problem

We assume a steady flow through two concentric cylinders of radii a and b ($a < b$). The flow is laminar and incompressible. A cylindrical polar coordinate system (r, φ, z) has been chosen and the common axis for both cylinders is z (as shown in Fig. 1). The rotating velocity of the outer cylinder is Ω as the inner cylinder is at rest. The rotation of the outer cylinder leads to the generation of the flow. The fluid flow depends on r only because the flow is fully developed. Both cylinders

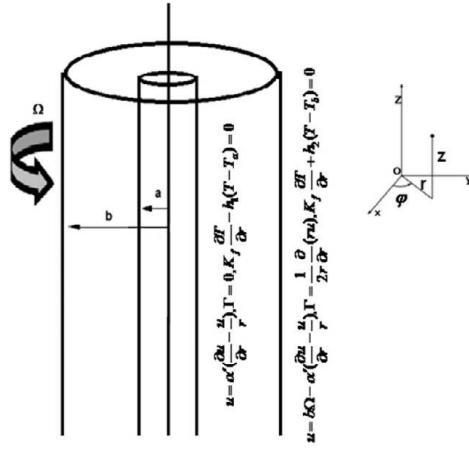


Figure 1. Classical representation of coordinate system

were considered with convective and slip boundary conditions. In addition, all the properties of the fluid are considered to be constant except for the density in the buoyancy term of the balance of momentum equation. Thus we have the following equations:

$$\frac{\partial u}{\partial \phi} = 0, \quad (1)$$

$$\mu \nabla_1^2 u + \rho g \beta_T (T - T_a) + \rho g \beta_C (C - C_a) = 0, \quad (2)$$

$$\alpha_1 \left(\frac{\partial^2 T}{\partial r^2} + \frac{1}{r} \frac{\partial T}{\partial r} \right) + \frac{\mu}{\rho C_p} \left(\frac{\partial u}{\partial r} - \frac{u}{r} \right)^2 + \frac{D_m K_T}{C_s C_p} \left(\frac{\partial^2 C}{\partial r^2} + \frac{1}{r} \frac{\partial C}{\partial r} \right) = 0, \quad (3)$$

$$D_m \left(\frac{\partial^2 C}{\partial r^2} + \frac{1}{r} \frac{\partial C}{\partial r} \right) + \frac{D_m K_T}{T_m} \left(\frac{\partial^2 T}{\partial r^2} + \frac{1}{r} \frac{\partial T}{\partial r} \right) - K_1 (C - C_a) = 0 \quad (4)$$

with

$$u = \alpha' \left(\frac{\partial u}{\partial r} - \frac{u}{r} \right), K_f \frac{\partial T}{\partial r} - s_1 (T - T_a) = 0, C = C_a, \quad (5a)$$

$$u = b\Omega - \alpha' \left(\frac{\partial u}{\partial r} - \frac{u}{r} \right), K_f \frac{\partial T}{\partial r} + s_2 (T - T_b) = 0, C = C_b. \quad (5b)$$

Here, α' is the slip length of the cylinders, s_1 is the convective heat transfer coefficient of the inner cylinder and s_2 is the convective heat transfer coefficient of the outer cylinder, T_a and T_b are the ambient temperatures, C_a and C_b are the

concentrations. Let u, v, w be the velocity components in x, y and z direction respectively, g^* is the gravity, K_f is the thermal diffusivity, ρ is the density, K_1 is the chemical reaction coefficient, C_s is the concentration susceptibility, C_p is the specific heat, μ is the viscosity, β_T is the thermal expansion, β_C is the solutal expansion, D_m is the mass diffusivity, T_m is the mean fluid temperature and K_T is the thermal diffusion ratio.

Introducing the following similarity variables

$$r = b\sqrt{\lambda}, u = \frac{\Omega}{\sqrt{\lambda}}f(\lambda), T - T_a = (T_b - T_a)\theta(\lambda), C - C_a = (C_b - C_a)\phi(\lambda), \quad (6)$$

substitute in equations (2) - (4), we get the governing dimensionless equations as

$$4\sqrt{\lambda}f'' + \frac{Gr_T}{Re}\theta + \frac{Gr_C}{Re}\phi = 0, \quad (7)$$

$$\lambda^3\theta'' + \lambda^2\theta' + Br(f - \lambda f')^2 + D_f Pr(\lambda^3\phi'' + \lambda^2\phi') = 0, \quad (8)$$

$$\lambda\phi'' + \phi' + ScSr(\lambda\theta'' + \theta') - \frac{K}{4}Sc\phi = 0 \quad (9)$$

with

$$-2\alpha\lambda_0 f'(\lambda_0) + (\sqrt{\lambda_0} + 2\alpha)f(\lambda_0) = 0, \quad (10a)$$

$$Bi_1\theta(\lambda_0) = 2\sqrt{\lambda_0}\theta'(\lambda_0), \phi(\lambda_0) = 0,$$

$$2\alpha f'(1) + (1 - 2\alpha)f(1) = b, Bi_2(1 - \theta(1)) = 2\theta'(1), \phi(1) = 1, \quad (10b)$$

where $\lambda_0 = (\frac{a}{b})^2$, $\alpha = \frac{a'}{b}$ is the slip coefficient, and $Bi_j = \frac{bs_j}{K_f}$ is the Biot number for inner and outer cylinders. Subindices $j = 1, 2$ refer to the inner and outer cylinders, respectively. In general, the Biot number is considered to be same for the two cylinders. The primes represent differentiation with respect to λ , $Re = \frac{\Omega b}{\nu}$

is the Reynolds number, $Gr_T = \frac{g\beta_T(T_b - T_a)d^3}{\nu^2}$ is the thermal Grashof number,

$Gr_C = \frac{g\beta_C(C_b - C_a)d^3}{\nu^2}$ is the solutal Grashof number, $Pr = \frac{\mu C_p}{K_f}$ is the Prandtl

number, $Br = \frac{\mu\Omega^2}{K_f(T_b - T_a)}$ is the Brinkman number, $Sc = \frac{\nu}{D}$ is the Schmidt

number, $Sr = \frac{D_m K_T (T_b - T_a)}{\nu T_m (C_b - C_a)}$ is the Soret number, $\alpha_1 = \frac{k}{\rho c_p}$ is the thermal

diffusivity, $D_f = \frac{D_m K_T (C_b - C_a)}{\nu C_p C_s (T_b - T_a)}$ is the Dufour number and $K = \frac{K_1 b^2}{\nu}$ is the chemical reaction parameter.

3 Solution of the problem

The initial approximations of the velocity ($f(\eta)$), temperature ($\theta(\eta)$) and concentration ($\phi(\eta)$) are chosen for HAM solutions as:

$$f_0(\lambda) = \frac{(-b\lambda_0\sqrt{\lambda_0}) + b(\sqrt{\lambda_0} + 2\alpha)\lambda}{\sqrt{\lambda_0}(1 - \lambda_0) + 2\alpha(1 + \lambda_0\sqrt{\lambda_0})},$$

$$\theta_0(\lambda) = \frac{2\sqrt{\lambda_0} - Bi\lambda_0 + Bi\lambda}{2(\sqrt{\lambda_0} + 1) + Bi(1 - \lambda_0)}, \quad \phi_0(\lambda) = \frac{\lambda - \lambda_0}{1 - \lambda_0}$$

and the auxiliary linear operator is

$$L_1 = \frac{\partial^2}{\partial \eta^2} \text{ such that } L_1(c_1\eta + c_2) = 0, \tag{11}$$

where c_1 and c_2 are the arbitrary constants. h_1 , h_2 and h_3 (control parameters of the convergence) are introduced in zero-order deformations.

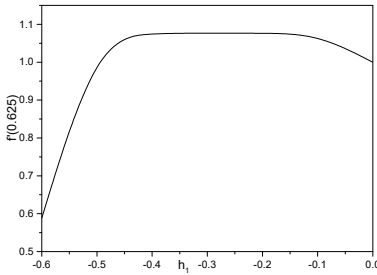


Figure 2. The h curve of $f(\lambda)$

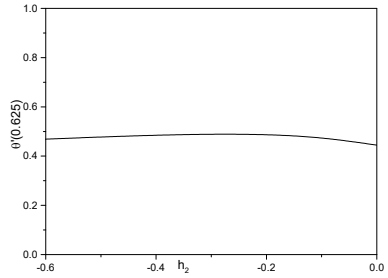


Figure 3. The h curve of $\theta(\lambda)$

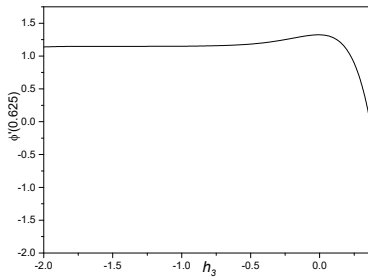


Figure 4. The h curve of $\phi(\lambda)$

The zero-order deformations; N_1 , N_2 and N_3 are non-linear operators; the average residual errors of f , θ and ϕ are considered as explained in the work of Kaladhar and Komuraiah [27]. h -curves are plotted with $Re = 2$, $Pr = 0.71$, $Sc = 0.22$, $Br = 0.5$, $Gr_T = 4$, $Gr_C = 4$, $Sr = 0.5$, $D_f = 0.5$, $K = 0.5$, $\alpha = 0.1$, $Bi = 0.5$, $b = 1$ for the optimal values of h_1 , h_2 and h_3 and are shown in Figs 2-4.

The admissible values of h_1 , h_2 and h_3 are evaluated as -0.34, -0.38, -1.34 respectively with the average residue errors (as explained in [27]) shown in Figs. 5-7.

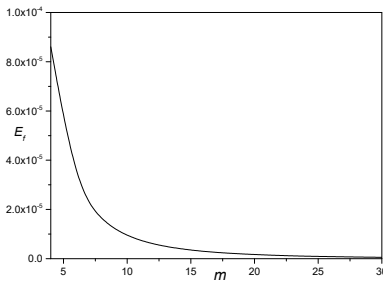


Figure 5. The average residual error of $f(\eta)$

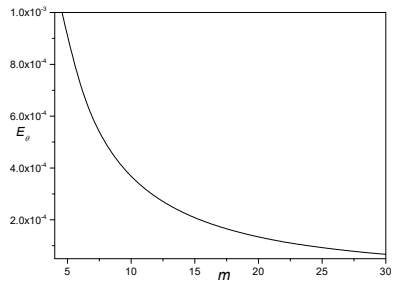


Figure 6. The average residual error of $\theta(\eta)$

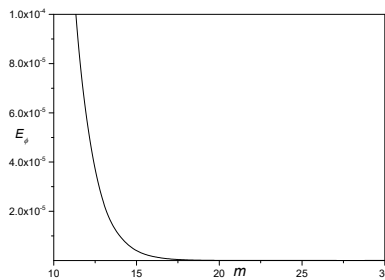


Figure 7. The average residual error of $\phi(\eta)$

Finally, the convergence of the series solutions is shown in Table 1.

Table 1. Convergence of HAM solutions for different orders of approximations

<i>Order</i>	$f(0.625)$	$\theta(0.625)$	$\phi(0.625)$
1	0.648787224	0.457261752	0.635687273
5	0.657163170	0.535762239	0.658236508
10	0.661828293	0.577323221	0.659072403
15	0.664098053	0.600093591	0.659047762
20	0.665556247	0.614893492	0.658011176
25	0.666587815	0.625409968	0.658987653
30	0.667359042	0.634628883	0.658987238
35	0.667490178	0.634629116	0.658987368
40	0.667490183	0.634629122	0.658987369
45	0.667490345	0.634629171	0.658987367
50	0.667490416	0.634629181	0.658987368

4 Results and Discussion

The profiles of velocity ($f(\lambda)$), temperature ($\theta(\lambda)$) and concentration ($\phi(\lambda)$) are computed and presented through plots in Figs. 8 to 20 with different values of Bi, α, Sr, D_f, K . Calculations were carried out by fixing the parameters $Re = 2, Pr = 0.71, Sc = 0.22, Br = 0.5, Gr_T = 4, Gr_C = 4, b = 1$ to analyze the effects of the emerging parameters Bi, α, Sr, D_f and K .

Figures 8-10 show the impact of Soret number (Sr) on f, θ and ϕ at $\alpha = 0.5, Bi=0.5, D_f=0.5, K=2$. It is shown from Fig. 8 that as Sr increases, the velocity of the fluid decreases by 16%. Since the values of Sr increase due to either decrease in the temperature difference or increase in the concentration difference. Therefore the velocity profiles decrease with the increase of the Soret number, i.e., the lowest peak of the reverse flow velocity compatible with the highest Soret parameter. It is seen from Fig. 9 that the temperature of the fluid diminishes by 24% as Sr increases. This is due to the flow heating vigorously with the decrease of the Soret parameter. It can be seen from Fig. 10 that the dimensionless concentration increases by 10% with the increase of Soret number. This is because of temperature gradients contribution to diffusion of the species. The present analysis shows that the flow field is appreciably influenced by the Soret number.

The impact of D_f on f, θ and ϕ can be seen in Figs. 11 to 13 at $\alpha = 0.5, Bi=0.5, Sr=0.5, K=0.5$. It is clear from Fig. 11 that the velocity diminishes by

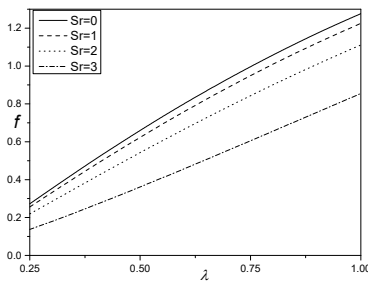


Figure 8. Soret effect on $f(\lambda)$

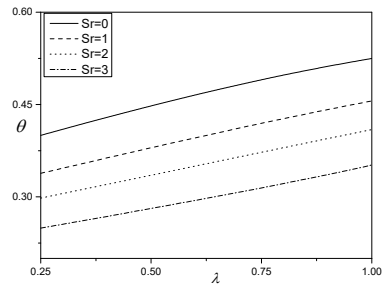


Figure 9. Soret effect on $\theta(\lambda)$

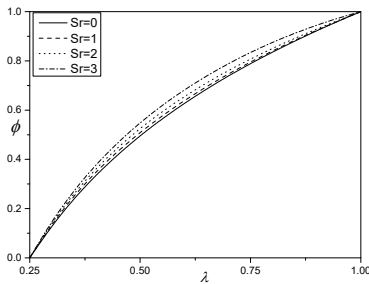


Figure 10. Soret effect on $\phi(\lambda)$

10% as D_f increases. Since the values of D_f increase due to either an increase in the temperature difference or decrease in the concentration difference, i.e., the lowest peak of the flow velocity compatible with the highest Dufour number. It is seen from Figs. 12-13 that the temperature of the fluid diminishes by 50% and the concentration of the fluid increases by 5% with an increase in D_f .

Figure 14 represents the influence of the chemical reaction parameter on the velocity profile $f(\eta)$ at $\alpha = 0.5$, $Bi=0.5$, $Sr=0.5$, $D_f=0.5$. It is seen from Fig. 14 that the velocity of the fluid increases by 10% as K increases. The impact of the chemical reaction parameter on the temperature profile can be found in Fig. 15. It is seen from Fig. 15 that the temperature of the fluid increases by 37% with an increase in K . Fig. 16 depicts the effect of the chemical reaction parameter on the concentration profile. These results clearly disclose that the flow field is decreased by 4% with the chemical reaction parameter. The higher K will decrease the concentration species.

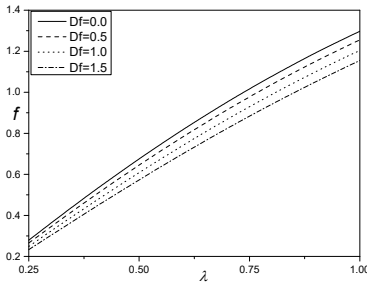


Figure 11. Dufour effect on $f(\lambda)$

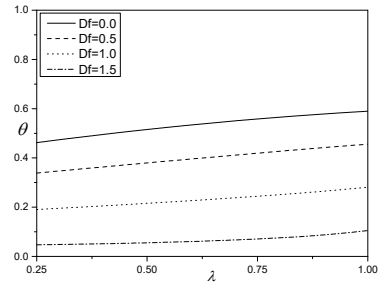


Figure 12. Dufour effect on $\theta(\lambda)$

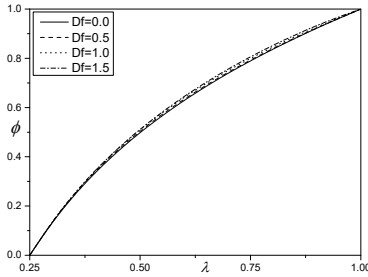


Figure 13. Dufour effect on $\phi(\lambda)$

The effect of the slip parameter α on f and θ can be seen in Figs. 17-18 at $K = 0.5, Bi=0.5, Sr=0.5, D_f=0.5$. It is noticed from Fig. 17 that the flow velocity increases by 43% with an increase in α . It is seen from Fig. 18 that the temperature of the fluid increases by 12% as α increases since the fluid friction decreases. The influence of Biot number Bi on f and θ can be seen in Figs. 19-20 at $K = 0.5, \alpha=0.5, Sr=0.5, D_f = 0.5$. Physically, Biot number is expressed as the convection at the surface of the body to the conduction within the surface of the body. Here we have assumed the convective heat transfer coefficients (s_1, s_2) are the same at the inner and outer cylinders, i.e., $Bi_1 = Bi_2 = Bi$. It is seen from Fig. 19 that the velocity of the fluid increases by 8% with an increase in Biot number. It is seen from Fig. 20 that an increase in Biot number leads to 43% increase in the temperature of the fluid.

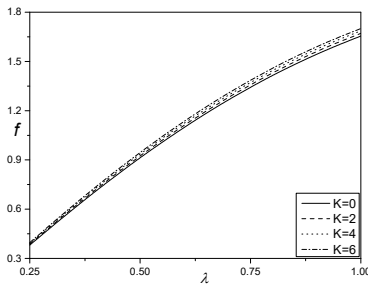


Figure 14. Chemical reaction effect on $f(\lambda)$

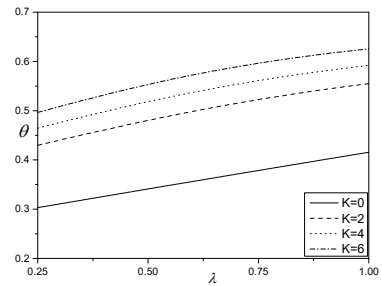


Figure 15. Chemical reaction effect on $\theta(\lambda)$

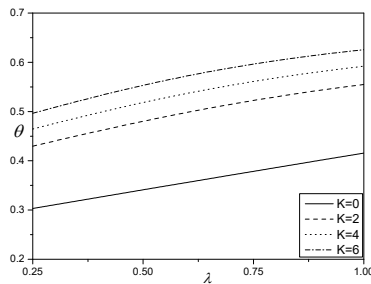


Figure 16. Chemical reaction effect on $\phi(\lambda)$

5 Conclusion

This study considered the steady natural convection flow of a Newtonian fluid in an annulus in the presence of cross diffusions and chemical reaction effects with Navier slip under convective boundary. Homotopy Analysis Method is used to find the final dimensionless governing equations. The significant conclusions are summarized as:

- Velocity and temperature profiles decrease whereas the concentration profile increases with an increase in Sr .
- The presence of Dufour parameter leads to decreases in the dimensionless temperature and velocity of the fluid but increases the concentration of the fluid.

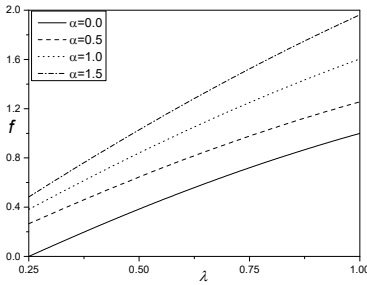


Figure 17. Slip parameter α effect on $f(\lambda)$

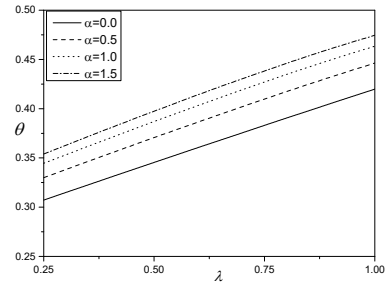


Figure 18. Slip parameter α effect on $\theta(\lambda)$

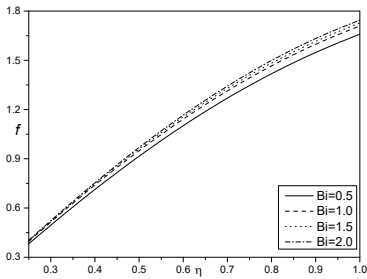


Figure 19. Effect of Biot number on $f(\lambda)$

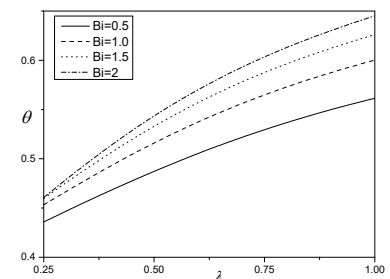


Figure 20. Effect of Biot number on $\theta(\lambda)$

- The velocity and temperature profiles increase while the concentration of the fluid decreases with the increase in the chemical reaction parameter.
- The flow velocity and temperature of the fluid increase with the increase of the slip parameter.
- The presence of the Biot number leads to an increase in velocity and temperature of the fluid.

Bibliography

[1] E. R. G. Eckert and W. O. Carlson, Natural convection in an air layer enclosed between two vertical plates with different temperatures, *International Journal of Heat and Mass Transfer* **2** (1961), 106–120.

- [2] B. Gebhart and L. Pera, The nature of vertical natural convection flows resulting from the combined buoyancy effects of thermal and mass diffusion, *International Journal of Heat and Mass Transfer* **14** (1971), 2025–2050.
- [3] T. H. Kuehn and R. J. Goldstein, Numerical solution to the Navier-Stokes equations for laminar natural convection about a horizontal isothermal circular cylinder, *International Journal of Heat and Mass Transfer* **23** (1980), 971–979.
- [4] T. Fusegi, J. M. Hyun, K. Kuwahara and B. Farouk, A numerical study of three-dimensional natural convection in a differentially heated cubical enclosure, *International Journal of Heat and Mass Transfer* **34** (1991), 1543–1557.
- [5] M. Y. Ha and M. J. Jung, A numerical study on three-dimensional conjugate heat transfer of natural convection and conduction in a differentially heated cubic enclosure with a heat-generating cubic conducting body, *International Journal of Heat and Mass Transfer* **43** (2000), 4229–4248.
- [6] A. Postelnicu, Influence of chemical reaction on heat and mass transfer by natural convection from vertical surfaces in porous media considering Soret and Dufour effects, *Heat and Mass Transfer* **43** (2007), 595–602.
- [7] M. Sheikholeslami and M. Shamlooei, $Fe_3O_4-H_2O$ nanofluid natural convection in presence of thermal radiation, *International Journal of Hydrogen Energy* **42** (2017), 5708–5718.
- [8] S. A. M. Mehryan, M. Ghalambaz and M. Izadi, Conjugate natural convection of nanofluids inside an enclosure filled by three layers of solid, porous medium and free nanofluid using Buongiorno's and local thermal non-equilibrium models, *Journal of Thermal Analysis and Calorimetry* **135** (2019), 1047–1067.
- [9] H. Ramkissoon and S. R. Majumdar, Unsteady flow of a micro-polar fluid between two concentric circular cylinders, *The Canadian Journal of Chemical Engineering* **55** (1977), 408–413.
- [10] F. S. Ibrahim, F. M. Hady, S. M. Abdel-Gaied and M. R. Eid, Influence of chemical reaction on heat and mass transfer of non-Newtonian fluid with yield stress by free convection from vertical surface in porous medium considering Soret effect, *Applied Mathematics and Mechanics* **31** (2010), 675–684.
- [11] O. D. Makinde, K. Zimba and O. A. Beg, Numerical study of chemically-reacting hydromagnetic boundary layer flow with Soret/Dufour effects and a convective surface boundary condition, *International Journal of Thermal and Environmental Engineering* **4** (2012), 89–98.
- [12] D. Srinivasacharya and K. Kaladhar, Mixed convection flow of chemically reacting couple stress fluid in a vertical channel with Soret and Dufour effects, *International Journal for Computational Methods in Engineering Science and Mechanics* **15** (2014), 413–421.

- [13] G. Nagaraju, M. Anjanna and K. Kaladhar, The effects of Soret and Dufour, chemical reaction, Hall and ion currents on magnetized micropolar flow through co-rotating cylinders, *AIP Advances* **7(11)** (2017), 115201 (1–16).
- [14] P. S. Reddy and A. Chamkha, Heat and mass transfer analysis in natural convection flow of nanofluid over a vertical cone with chemical reaction, *International Journal of Numerical Methods for Heat and Fluid Flow* **27** (2017), 2–22.
- [15] G. Nagaraju, J. Srinivas, J. V. Ramana Murthy, O. A. Beg and A. Kadir, Second law analysis of flow in a circular pipe with uniform suction and magnetic field effects. *ASME. J. Heat Transfer* **141(1)** (2019), 012004 (1–9).
- [16] S. Jain and R. Choudhary, Soret and Dufour effects on thermophoretic MHD flow and heat transfer over a non-linear stretching sheet with chemical reaction, *International Journal of Applied and Computational Mathematics* **4** (2018), 50 (1–27).
- [17] M. A. A. Hamad, Analytical solution of natural convection flow of a nanofluid over a linearly stretching sheet in the presence of magnetic field, *International Communications in Heat and Mass Transfer* **38** (2011), 487–492.
- [18] W. N. Mutuku-Njane and O. D. Makinde, Combined effect of Buoyancy force and Navier slip on MHD flow of a nanofluid over a convectively heated vertical porous plate, *The Scientific World Journal* **2013** (2013), Article ID 725643.
- [19] B. Prabhakar, S. Bandari and C. Kumar, Effects of inclined magnetic field and chemical reaction on flow of a Casson Nanofluid with second order velocity slip and thermal slip over an exponentially stretching sheet, *International Journal of Applied and Computational Mathematics* **3** (2017), 2967–2985.
- [20] M. Usman, T. Zubair, M. Hamid, R. Haq and W. Wang, Wavelets solution of MHD 3-D fluid flow in the presence of slip and thermal radiation effects, *Physics of Fluids* **30** (2018), 023104.
- [21] D. Srinivasacharya and K. Hima Bindu, Entropy generation due to micropolar fluid flow between concentric cylinders with slip and convective boundary conditions, *Ain Shams Engineering Journal* **9(2)** (2018), 245–255.
- [22] M. Waleed Ahmad Khan, M. Ijaz Khan, T. Hayat and A. Alsaedi, Numerical solution of MHD flow of power law fluid subject to convective boundary conditions and entropy generation, *Computer Methods and Programs in Biomedicine* **188** (2020), 105262, <https://doi.org/10.1016/j.cmpb.2019.105262>.
- [23] Chein-Shan Liu, Lin Qiu and J. Lin, Solving heat equations under convection boundary conditions by a high-performance space-time boundary shape functions method, *Numerical Heat Transfer, Part B: Fundamentals* **77(4)** (2020), 311–327.
- [24] Z. Ziabakhsh and G. Domairry, Analytic solution of natural convection flow of a non-Newtonian fluid between two vertical flat plates using homotopy analysis method, *Communications in Nonlinear Science and Numerical Simulation* **14** (2009), 1868–1880.

- [25] A. R. Sohoul, M. Famouri, A. Kimiaefar and G. Domairry, Application of homotopy analysis method for natural convection of Darcian fluid about a vertical full cone embedded in porous media prescribed surface heat flux, *Communications in Nonlinear Science and Numerical Simulation* **15** (2010), 1691–1699.
- [26] C. S. Sravanthi, Homotopy analysis solution of MHD slip flow past an exponentially stretching inclined sheet with Soret-Dufour effects, *Journal of the Nigerian Mathematical Society* **35** (2016), 208–226.
- [27] K. Kaladhar and E. Komuraiah, Homotopy analysis for the influence of Navier slip flow in a vertical channel with cross diffusion effects, *Mathematical Sciences* **11** (2017), 219–229.
- [28] A. K. Ray, B. Vasu, P. V. S. N. Murthy and R. S. R. Gorla, Non-similar solution of Eyring-Powell fluid flow and heat transfer with convective boundary condition: Homotopy analysis method, *Int. J. Appl. Comput. Math* **6** (2020), <https://doi.org/10.1007/s40819-019-0765-1>.

Received November 19, 2020; revised March 25, 2020; accepted June 22, 2020.

Author information

Kolla Kaladhar, Department of Mathematics, National Institute of Technology Warangal, India.

E-mail: kaladhar@nitw.ac.in

Eerala Komuraiah, Department of Mathematics, National Institute of Technology Puducherry, India.

E-mail: ek.nitpy@gmail.com

Kothakapu Madhusudhan Reddy, Department of Mathematics, National Institute of Technology Puducherry, India.

E-mail: madhu.nitpy@gmail.com